

Selective Photorearrangement of 1-(2-Naphthoyl)aziridine to 2-(2-Naphthyl)-2-oxazoline by Polybromobenzenes

Sei-ichi Nishimoto, Tsukuru Izukawa, and Tsutomu Kagiya *

Department of Hydrocarbon Chemistry, Faculty of Engineering, Kyoto University, Kyoto 606, Japan

Photoreactions of 1-(2-naphthoyl)aziridine (1) in the presence of various brominated hydrocarbons (4a–f) in deaerated benzene solution have been studied at room temperature. The selective photorearrangement of (1) to 2-(2-naphthyl)-2-oxazoline (2) was promoted by 1,3,5-tribromobenzene (4a) and 1,4-dibromobenzene (4b). The nonpolar solvent benzene favoured selective photorearrangement, compared with polar acetonitrile. The series of brominated hydrocarbons (4a–e) but not $\text{CH}_3(\text{CH}_2)_2\text{Br}$ (4f) formed 1:1 ground-state complexes with (1). The fluorescence emission of (1) was quenched efficiently by (4a–f). The fluorescence-quenching rate constant (k_q) increased on increasing the half-wave reduction potential ($E^{\text{Red}}_{\frac{1}{2}}$) of (4a–f). The photosensitized triplet reaction of (1) did not give (2) but a small amount of oligomer. The reciprocal of the quantum yield for the photorearrangement (Φ^{-1}) was proportional to that of the concentration of non-complexed (4a) $\{[(4a)]_{\text{free}}\}^{-1}$.

Although the thermal reactivities of three-membered aziridines have been well characterized,¹ their photochemical behaviour have been little explored.² In a preliminary study on the photoreactions of 1-(2-naphthoyl)aziridine (1) in various solvents, we observed photochemical ring opening of the aziridinyl moiety of (1) at the C–N bond to give secondary amide derivatives.³ In these photoreactions solvent molecules also react to determine whether the ring opening occurs by a radical or an ionic mechanism.³ Another interesting characteristic of the solvent effects was the fact that irradiation in CH_2Br_2 led to rearrangement of (1) to 2-(2-naphthyl)-2-oxazoline (2) in fairly good yield as well as the major ring-opening reaction into *N*-(2-bromoethyl)naphthalene-2-carboxamide (3).

In this paper we report our further finding that polybromobenzenes promote selective photorearrangement of (1) to (2) in nonpolar benzene solution under deaerated conditions. The photorearrangement mechanism is discussed on the basis of the behaviour of the brominated hydrocarbons in the ground-state complex formation, the fluorescence quenching, and the photosensitized triplet reaction of (1).

Experimental

Materials.—1-(2-Naphthoyl)aziridine (1) was prepared and purified as reported.³ 1,3,5-Tribromobenzene (4a) and 1,4-dibromobenzene (4b) were purified by recrystallization from chlorobenzene. Bromobenzene (4c), dibromomethane (4e), propyl bromide (4f), and allyl bromide (4g) were fractionally distilled before use. Bromoform (4d) (spectroscopic grade) and carbon tetrabromide (4h) were used as received. Benzene was of spectroscopic grade and used without further purification. Acetonitrile was refluxed over phosphorus pentoxide and then fractionally distilled before use. Benzophenone, anthraquinone, flavone, and Michler's ketone were used as received.

Spectroscopic Measurements.—Electronic absorption spectra were recorded on a Shimadzu UV-200S spectrophotometer. Fluorescence spectra were measured at room temperature by a JASCO FP-550A fluorescence spectrophotometer. The spectral response over the wavelength region for the measurements was corrected by a standard tungsten lamp. The fluorescence lifetime of 0.6mM-(1) in deaerated benzene solution was determined by a single-photon time coincidence method with an ORTEC 9200 nanosecond fluorimeter and a Hitachi multichannel analyser.⁴ Pulsed light with a half-duration of *ca.* 2.5 ns was generated by a

spark discharge in air across tungsten electrodes. The phosphorescence spectra of 0.5mM-(1) in EP glass (50% v/v diethyl ether–isopentane) were recorded at 77 K on a Hitachi MPF-4 phosphorescence spectrophotometer.

Photoreactions.—Typically, a solution containing 0.09mM-(1) and 0.2M-brominated hydrocarbon in benzene (1 ml) was prepared in a Pyrex glass tube (6 mm diameter, cut-off wavelengths below 286 nm), deaerated by repeated freeze–pump–thaw cycles under reduced pressure (<40 mPa), and then sealed before irradiation. Irradiation was performed at room temperature with a merry-go-round apparatus equipped with a 400 W high-pressure mercury arc (Eiko-sha 400). The calibrated emission spectrum of the light source was obtained with a JASCO CT-25N monochromator and a vacuum thermopile. The absolute light intensity at 313 nm was determined as 1.10×10^{-7} einstein $\text{ml}^{-1} \text{min}^{-1}$ with a ferrioxalate actinometer ($\Phi_{\text{Fe(II)}}$ 1.24 at 313 nm).⁵ Under these conditions of photoreaction, the influence of exciting the brominated hydrocarbon was estimated as <0.05% relative to uncomplexed and complexed (1).

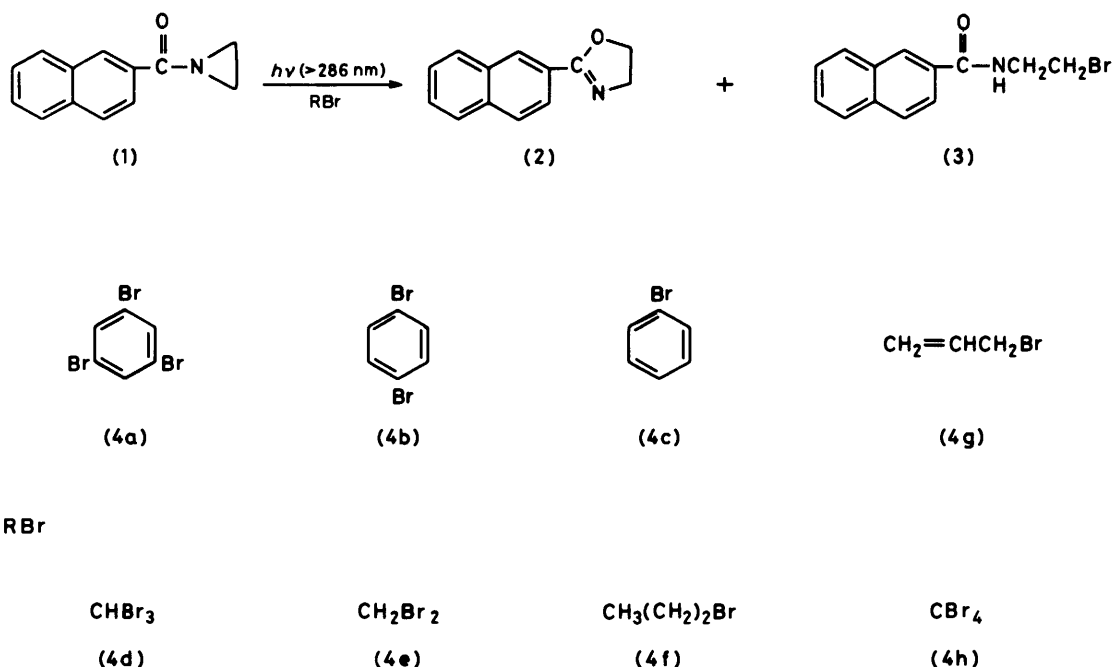
The photoproducts obtained after evaporation of the benzene were subjected to ¹H n.m.r. measurement on a JEOL PMX-60 spectrometer with tetramethylsilane as internal standard and h.p.l.c. analysis with a TOYO SODA HLC-802UR high-performance liquid chromatograph using the column conditions reported.³ The quantum yield for the photoreaction (Φ) was obtained as the ratio of the initial rate of product formation to the initial number of quanta absorbed by the reaction system. The light intensities in the wavelength range effective for the photoreaction were estimated from the emission spectrum by reference to the absolute value at 313 nm.

Oxidation and Reduction Potentials.—The oxidation potential ($E^{\text{Ox}}_{\frac{1}{2}}$) of (1) and the reduction potential ($E^{\text{Red}}_{\frac{1}{2}}$) of (4a) were evaluated relative to a saturated calomel electrode (s.c.e.) by means of cyclic voltammetry (c.v.) for the argon-saturated acetonitrile solution (0.01M) containing 1M-sodium perchlorate as a supporting electrolyte. Cyclic voltammograms were measured with a Hokuto Denki HB-104 voltage scanner and a Hokuto Denki HA-104 potentiostat. Glassy carbon and platinum coil were used as the working and auxiliary electrodes, respectively. Since the current–potential curves in both cases exhibited irreversible peaks, the half-peak potentials were used to estimate the values for $E^{\text{Ox}}_{\frac{1}{2}}$ of (1) and $E^{\text{Red}}_{\frac{1}{2}}$ of (4a).

Table 1. Photoreactions of 0.09M-(1) in benzene solutions containing 0.2M-brominated hydrocarbons ^a

Brominated hydrocarbon	Irradiation time (min)	Conversion (%)	Φ^b	Product selectivity (%) [yield (%)]		
				(2)	(3)	Oligomer ^c
None	200	6	0.004	0 (0)	0 (0)	100 (6)
1,3,5-C ₆ H ₃ Br ₃ (4a)	200	100	0.062	91 (91)	0 (0)	9 (9)
1,4-C ₆ H ₄ Br ₂ (4b)	200	91	0.056	90 (82)	7 (6)	3 (3)
C ₆ H ₅ Br (4c)	200	20	0.009	65 (13)	30 (6)	5 (1)
CHBr ₃ (4d)	48	31	0.051	57 (18)	43 (13)	0 (0)
CH ₂ Br ₂ (4e)	100	29	0.033	82 (24)	11 (3)	7 (2)
CH ₃ CH ₂ CH ₂ Br (4f)	200	18	0.002	15 (3)	54 (10)	31 (5)

^a On irradiation through a Pyrex glass tube ($\lambda_{\text{ex.}} > 286 \text{ nm}$) at room temperature. ^b Quantum yield for the formation of (2). ^c Yield based on (1).

**Scheme 1.**

Results and Discussion

Characteristics of the Photoreaction.—Table 1 summarizes the effects of a series of brominated hydrocarbons (4a–f) on the photoreactivity of (1) and the product distribution. It is seen from Table 1 that (1) undergoes rearrangement to (2) along with a ring-opening reaction to give the bromine-substituted primary amide (3) when irradiated in the presence of (4a–f) in deaerated benzene solution.

Although (1) was virtually stable to exposure at $\lambda_{\text{ex.}} > 286 \text{ nm}$ in deaerated benzene, its conversion was remarkably enhanced by the addition of (4a–f), increasing with increased bromine substitution. Increasing bromine substitution also tended to increase the yield of (2) as a major product. In particular, polybromobenzenes such as (4a and b) led to the formation of (2) with a selectivity of $>90\%$.

The yields of the ring-opened product (3) were high in the presence of (4c–f), but their selectivities were $<54\%$ at the relatively low conversion ($\lesssim 30\%$) of (1). It should be noted that the selectivity of the formation of (3) in each of these systems increased as the irradiation was prolonged. This behaviour can be accounted for by the fact that not only (1) but also the primary product of (2) is subsequently converted into (3) *via* photochemical ring-opening reaction with bromin-

ated hydrocarbons.⁶ In contrast to (4c–f), both (4a and b) brought about the linear increase in the yield of (2) with irradiation time. The quantum yields for the photorearrangement of (1) estimated at the initial stage of irradiation were also listed in Table 1, indicating that the bromobenzene series is more effective for the photorearrangement than the bromoalkane series with the same number of bromine substituents.

Figure 1 shows the effect of solvent polarity on the photorearrangement of (1) (0.09M) in the presence of 0.2M-(4a), which was determined for benzene–acetonitrile mixtures. The Φ value for the photorearrangement is seen not to vary significantly with dielectric constant of the mixed solvent (ϵ). It is, however, remarkable that as ϵ increases the selectivity of rearrangement decreases appreciably because of the enhanced oligomerization. This result indicates that nonpolar solvents favour the photorearrangement of (1) by brominated hydrocarbons.

Ground-state Complex Formations of (1) with Brominated Hydrocarbons.—From the electronic spectral change, the photoreaction system was found to involve the complex formation between (1) and the brominated hydrocarbon in their ground states. Figure 2 illustrates a typical difference-absorption spectrum of the mixture of 0.4mM-(1) and 0.57M-

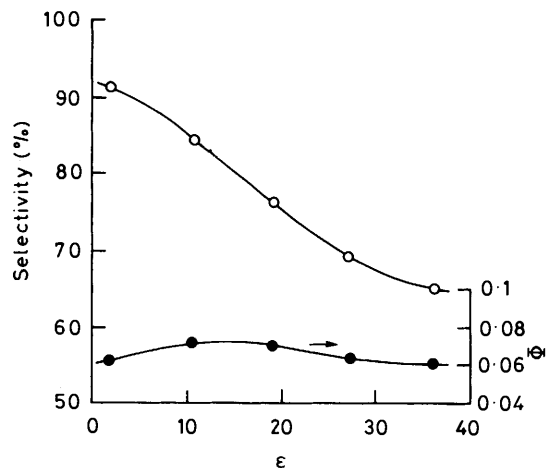


Figure 1. Variations in ●, quantum yield and ○, selectivity for the photorearrangement of 0.09M-(1) to (2) in the presence of 0.2M-(4a) with dielectric constant of benzene-acetonitrile mixed solvent [$\epsilon = 2.275v_{C_6H_6} + 35.95(1 - v_{C_6H_6})$, where $v_{C_6H_6}$ is the volume fraction of benzene]

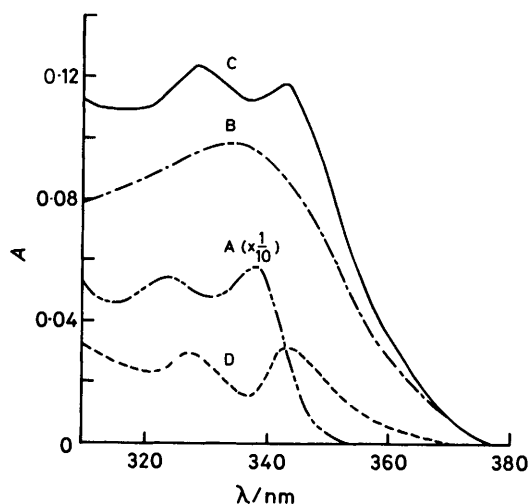
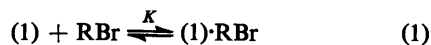


Figure 2. Electronic absorption spectra of A, 0.4mM-(1) and B, 0.57mM-(4b) in benzene, both with reference to the benzene solvent, the difference absorption spectrum of C, the mixture of 0.4mM-(1) and 0.57mM-(4b) in benzene (sample solution) with reference to the benzene solution of 0.4mM-(1), and the apparent absorption spectrum of D, a 1:1 complex between (1) and (4b) which was obtained by subtracting B from C

(4b) in benzene observed by reference to the corresponding benzene solution of (1) without (4b). For comparison, the absorption spectra characteristic of the individual components are also shown in Figure 2. These spectral data clearly demonstrate the appearance of a new absorption band which was attributable to a 1:1 complex of (1) with (4b) (see Figure 3). Similar results were obtained with the other brominated hydrocarbons except for (4f).

We attempted to determine the equilibrium constant (K) by assuming a 1:1 complex formation of (1) with a given brominated hydrocarbon (RBr). With a large excess of RBr



relative to (1) $\{[RBr]_0 \gg [(1)]_0 > [(1) \cdot RBr]\}$, the Benesi-Hildebrand equation⁷ is represented by (2) where $\epsilon_1(\lambda)$ and

$$\frac{l[(1)]_0}{\Delta A(\lambda)} = \frac{1}{[\epsilon_c(\lambda) - \epsilon_1(\lambda)]} + \frac{1}{K[\epsilon_c(\lambda) - \epsilon_1(\lambda)]} \cdot \frac{1}{[RBr]_0} \quad (2)$$

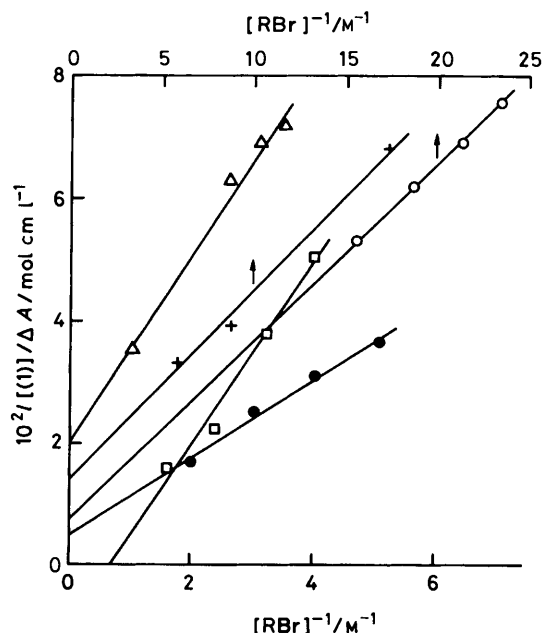


Figure 3. Illustration of the Benesi-Hildebrand plots for the formation of the 1:1 complex of (1) with various brominated hydrocarbons (RBr) in benzene solution at room temperature: ○, (4a) at 360 nm; +, (4b) at 313 nm; △, (4c) at 313 nm; ●, (4d) at 340 nm; □, (4e) at 340 nm

Table 2. Ground-state complex formation and fluorescence quenching of (1) in the presence of brominated hydrocarbons in benzene solution at room temperature

Brominated hydrocarbon	$-E^{Red}_{\frac{1}{2}}$ ^a / V vs. s.c.e.	K ^b / l mol ⁻¹	$10^{-8}k_q$ ^c / l mol ⁻¹
1,3,5-C ₆ H ₃ Br ₃ (4a)	1.61 ^d	2.3	90
1,4-C ₆ H ₄ Br ₂ (4b)	2.10	2.3	35
C ₆ H ₅ Br (4c)	2.32	1.4	2.2
CHBr ₃ (4d)	0.64	0.9	66
CH ₂ Br ₂ (4e)	1.48	<0	7.9
CH ₃ CH ₂ CH ₂ Br (4f)	2.20 ^e	<i>f</i>	1.6
CH ₂ =CHCH ₂ Br (4g)	1.29		120
CBr ₄ (4h)	0.3		110

^a I. M. Kolthoff and J. J. Lingane, 'Polarography,' Interscience, New York, 1952, vol. II, p. 647. ^b Equilibrium constant for ground-state complex formation. ^c Rate constant of fluorescence quenching of (1) evaluated with 313 nm excitation under deaerated conditions. ^d Obtained by c.v. in acetonitrile. ^e F. L. Lambert and K. Kobayashi, *J. Am. Chem. Soc.*, 1960, 82, 5324. ^f Complex formation was not observed.

$\epsilon_c(\lambda)$ are molar extinction coefficients of (1) and the complex at wavelength λ , respectively, l is the light-path length, and $\Delta A(\lambda)$ is the apparent absorbance of the complex band at λ defined as the difference in absorbance between the solutions before and after mixing, i.e. $\Delta A = A(\text{mixture}) - A\{(1)\} - A(RBr)$ (see also Figure 2). Figure 3 shows linear relationships resulting from the Benesi-Hildebrand plots obtained for a fixed concentration of (1) with varying concentrations of (4a-e). These plots are consistent with the 1:1 complex formation as assumed in equation (1).

The average K value for each system was derived from the Benesi-Hildebrand plots at three different wavelengths and is listed in Table 2. A negative K value (-0.76 l mol⁻¹) was obtained only in the case of (4e). Since polyhalogenomethanes

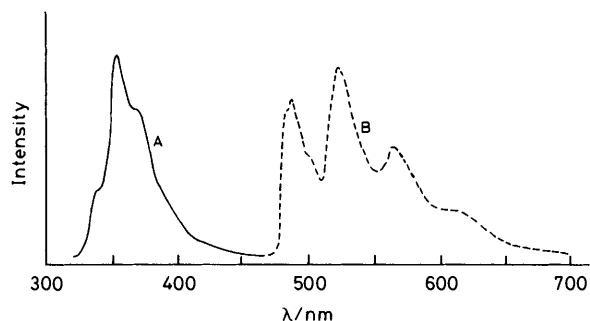


Figure 4. Emission spectra of (1): A, fluorescence in benzene (0.4 mM) at room temperature; B, phosphorescence in 50% v/v diethyl ether-isopentane (0.5 mM) at 77 K

are known to form 1 : 1 complexes with benzene,⁸ the possible complexation of (4e) with the benzene solvent would lead to a serious error in the determination of the K value in this system. This influence of the benzene solvent is also probably involved in the other systems, but a trend is evident in Table 2 in that the K value increases with the increased reduction potential $E^{\text{Red}}_{1/2}$ for the bromobenzene series and the bromoalkane series, respectively.* On the other hand, although the distinct complex-band maxima could not be obtained for all systems, the enhanced red shift of the complex band was observed upon increasing the $E^{\text{Red}}_{1/2}$ value which was larger in the bromobenzene series. These results suggest that there is a significant charge-transfer interaction between (1) and the brominated hydrocarbon in ground-state complex formation.

Photoreactivity of the Ground-state Complex.—In order to characterize the photochemical behaviour of the ground-state complex, a deaerated benzene solution containing 0.02 M-(1) and 0.2 M-(4a) was irradiated with a combination of Toshiba UV-DIB and V-40 glass filters (a maximum transmittance of 17.7% at 366 nm and 326–392 nm band-pass). After irradiation for 23 h formation of (2) (13% yield) and (3) (21% yield) was observed. Since the direct photoexcitation of (1) should be minor under these conditions, these products seem not to be due to the reaction of (1) in its electronically excited states. On the other hand, (1) (0.02 M) was confirmed to undergo a dark ring-opening reaction to give a 19% yield of (3) in the benzene solution of 0.2 M-(4a) irradiated under similar conditions prior to the addition of (1). In this postreaction system, however, the rearrangement of (1) to (2) did not occur. Although the participation of a bimolecular reaction between (1) in the ground state and (4a) in the excited state cannot be ruled out at the present stage, it is likely that excitation of the 1 : 1 complex between (1) and (4a) in their ground states leads to the formation of (2).

Fluorescence Quenching.—A deaerated benzene solution of 0.4 mM-(1) showed the intense fluorescence emission with vibrational structures at 340, 356, and 371 nm (Figure 4). The fluorescence lifetime (τ^0_f) of (1) under these conditions was measured as 15.5 ns by the single-photon counting method. The addition of (4a–f) resulted in quenching of the fluorescence emission without change in spectral profile. As shown in Figure 5, the Stern–Volmer plot gave a straight line for each

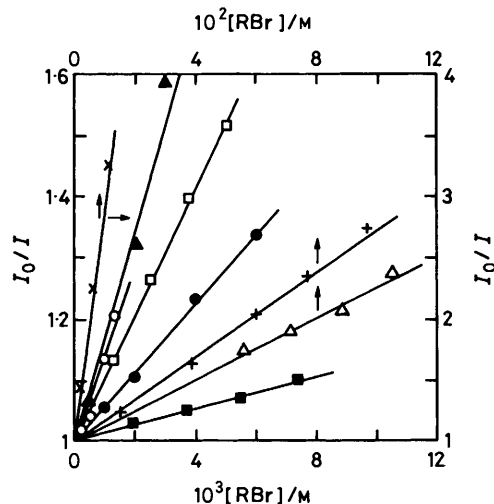


Figure 5. Stern–Volmer plots for the fluorescence quenching of 0.4 mM-(1) by various brominated hydrocarbons (RBr) in deaerated benzene solution at room temperature: O, (4a); ●, (4b); +, (4c); □, (4d); ■, (4e); △, (4f); ▲, (4g); ×, (4h)

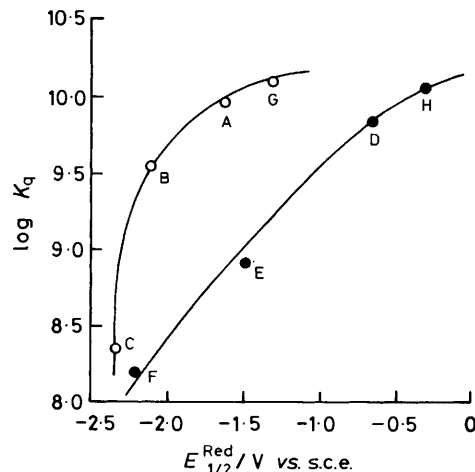
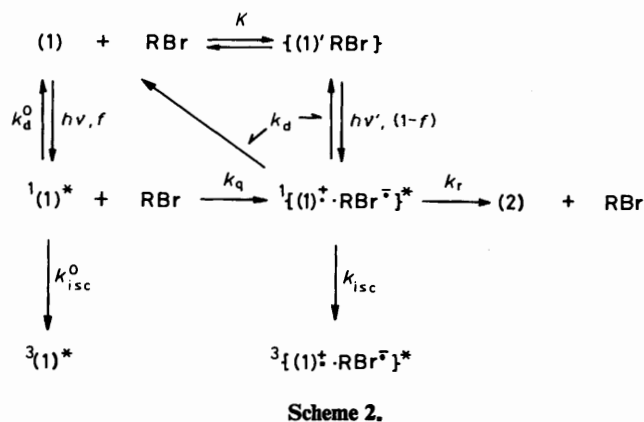


Figure 6. Variation in log (fluorescence-quenching rate constant) ($\log k_q$) as a function of the half-wave reduction potential ($E^{\text{Red}}_{1/2}$) for O, the bromobenzene series and ●, the bromoalkane series; A, (4a); B, (4b); C, (4c); D, (4d); E, (4e); F, (4f); G, (4g); H, (4h)

of (4a–f). In the case of (4c) a relatively large amount was required for the efficient fluorescence quenching of (1) and therefore corrections were made in the Stern–Volmer plot to eliminate the influences of both the spectral overlap and the ground-state complexation. Such influences were considered as minor in the other systems. The fluorescence-quenching rate constants (k_q) were evaluated from the τ^0_f value and the slopes ($= k_q \tau^0_f$) of the Stern–Volmer plots. The numerical results are summarized in Table 2, together with the data obtained for (4g and h).

In Figure 6, $\log k_q$ is plotted as a function of $E^{\text{Red}}_{1/2}$ for a series of brominated hydrocarbons (4a–h). It is noteworthy in Figure 6 that the $E^{\text{Red}}_{1/2}$ dependence of k_q for the bromobenzene series including (4g) with π orbitals is significantly different from the bromoalkane series. Thus, with the increase in $E^{\text{Red}}_{1/2}$, the k_q value in the bromobenzene series increases more rapidly to attain a diffusion-limit value than the bromoalkane series. This is very similar to their behaviour in the ground-state complexation. The $E^{\text{Red}}_{1/2}$ dependence of k_q

* The difference in complexation behaviour between bromobenzene series and bromoalkane series may be interpreted by assuming that the π - π interaction with (1) is predominant in the complexation for the former series whereas the π - σ interaction predominates for the latter series.



also suggests that an electron-transfer (or charge-transfer) process between (1) in the lowest excited singlet state (S_1)^{*} and (4a—g) is responsible for the fluorescence quenching.[†]

Reaction Characteristics of (1) in the Triplet State.—The phosphorescence spectrum of 0.5mM-(1) measured in EP glass at 77 K had the vibrational structures at 488 (0—0 band), 524, and 565 nm (Figure 3). Since the spectral profile of (1) is very similar to that of the parent naphthalene, the lowest triplet state (T_1) of (1) is suggested to be of a $^3(\pi, \pi^*)$ state. Furthermore, the T_1 energy level (E_T) of (1) is estimated as 245 kJ mol⁻¹ from the phosphorescence 0—0 band (20 500 cm⁻¹).

The photosensitized triplet reactions of 0.1M-(1) in deaerated benzene solution were also attempted with various sensitizers (0.01M) having E_T values larger than 245 kJ mol⁻¹, e.g. benzophenone (E_T 287 kJ mol⁻¹),¹⁰ anthraquinone (261),¹⁰ flavone (259),¹⁰ and Michler's ketone (255).¹⁰ On irradiation for 10 h at $\lambda_{ex.} > 286$ nm in each reaction system, only the oligomerization of (1) could be observed, in less than 7% yield. Selective excitation of 0.01M-anthraquinone in deaerated benzene solution containing 0.01M-(1) and 0.2M-(4b) for 10 h with the use of a Toshiba L-42 filter ($\lambda_{ex.} > 350$ nm) could also induce no reaction of (1).[‡]

In view of these results, it seems that neither a unimolecular triplet reaction nor bimolecular triplet quenching by (4a—f) is responsible for the rearrangement of (1) to (2). Thus, if the efficient fluorescence quenching by (4a—f) (Table 2) is only due to the enhanced $S_1 \rightarrow T_1$ intersystem crossing of (1), the quantum yield of the photorearrangement should decrease with the increase in k_q value. Clearly, this is not the case for the present photoreaction systems.

Mechanism of the Photorearrangement.—From the results described above we conclude that the photorearrangement of (1) involves its S_1 state undergoing electron-transfer quenching by brominated hydrocarbons (dynamic path) as is shown in Scheme 2. It is presumed that the three-membered aziridinylium moiety of the resulting cation radical of (1) is labile and undergoes a ring-opening reaction at the C—N bond followed

* The S_1 state of (1) is not a $^1(n, \pi^*)$ state but a $^1(\pi, \pi^*)$ state³ with energy of 353 kJ mol⁻¹.

† The free-enthalpy change (ΔG_{et}) of electron transfer from the S_1 state of (1) to (4a) in acetonitrile was estimated as -52.6 kJ mol⁻¹ on the basis of the Rehm-Weller equation⁹ with the values of $E^{ox}_{\frac{1}{2}}\{(1)\} = 1.56$ V versus s.c.e. and $E^{red}_{\frac{1}{2}}\{(4a)\} = -1.61$ V versus s.c.e. obtained by c.v. in acetonitrile.

‡ Since the T_1 energy level of (4b) (E_T 334 kJ mol⁻¹)¹¹ lies sufficiently above that of anthraquinone, the photosensitization in this system should produce exclusively the T_1 state of (1).

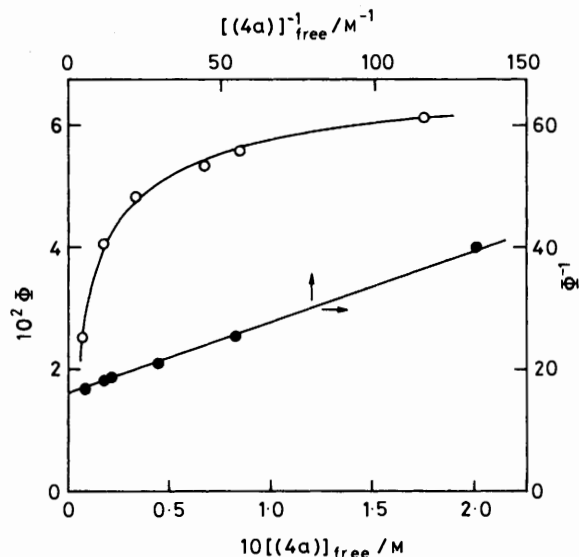


Figure 7. Variation in quantum yield for the photorearrangement (Φ) of 0.09M-(1) in deaerated benzene solution as a function of the concentration of noncomplexed (4a) $\{[(4a)]_{free}\}$, estimated with the equilibrium constant (K) listed in Table 2

by ring closure to give a five-membered oxazoline. The rearrangement is completed by a back-electron-transfer from the anion radical of the brominated hydrocarbon to the cation radical of (2) thus formed. Benzene favours these reaction processes if they proceed *via* a cation radical-anion radical pair, because ionic dissociation is depressed in nonpolar solvents. This is consistent with the observed solvent effect on the photorearrangement. In the case of the rearrangement of (1), by exciting the ground-state complexes with brominated hydrocarbons, enhanced electron-transfer reaction can also occur intramolecularly within the complex (static path) to produce a similar ion radical pair (Scheme 2).

Following Scheme 2, the quantum yield for the photorearrangement is given by equation (3) where f is the fraction

$$\Phi = \frac{k_r}{k_d + k_{1.s.c.} + k_r} \left[\frac{fk_q[\text{RBr}]_{free}}{k_d^0 + k_{1.s.c.}^0 + k_q[\text{RBr}]_{free}} + (1-f) \right] \quad (3)$$

of light absorption by noncomplexed (1) and $[\text{RBr}]_{free}$ is the concentration of noncomplexed brominated hydrocarbon. As is seen from equation (3), both the dynamic and the static paths make contributions to the observed Φ value. In order to evaluate the relative contributions from the two paths, the Φ values were determined in deaerated benzene solution for a fixed concentration of (1) (0.09M) and by varying the concentration of (4a) up to 0.2M. Figure 7 shows a plot of Φ versus $[(4a)]_{free}$. It is also noted in Figure 7 that the reciprocal of the Φ value is proportional to that of $[(4a)]_{free}$. This linear relationship agrees with a special case of equation (3) in which the static path is neglected. Thus, the rearrangement of (1) under these conditions occurs almost exclusively *via* the dynamic quenching of the S_1 state of (1) by (4a). From the slope and the intercept of the straight line in Figure 7 we can obtain the values of $k_r/(k_d + k_{1.s.c.} + k_r) = 0.062$ and $k_q/(k_d^0 + k_{1.s.c.}^0) = k_q\tau_f^0 = 94$ l mol⁻¹ by reference to equation (3). The $k_q\tau_f^0$ value thus obtained is smaller than that of the fluorescence-quenching data (140 l mol⁻¹), but the agreement is considered reasonable.

Since Scheme 2 does not involve the ring-opening reaction to give (3), it takes in only the selective photorearrangement to (2) as in the case when using (4a or b). Nevertheless, the essential part of the ring-opening reaction mechanism is described by Scheme 2. We can predict that the less stable anion radical of the brominated hydrocarbon leads to more efficient formation of (3).

Acknowledgements

We thank Professor Y. Nishijima and Dr. S. Ito for the fluorescence lifetime measurements and Associate Professor Y. Wada for the phosphorescence measurements.

References

- 1 O. C. Dermer and G. F. Hamm, 'Ethylenimine and Other Aziridines,' Academic Press, New York, 1969; C. U. Pittman, Jr., S. P. McManus, and J. W. Larsen, *Chem. Rev.*, 1972, **72**, 357; S. P. McManus, R. A. Hearn, and C. U. Pittman, Jr., *J. Org. Chem.*, 1976, **41**, 1895.
- 2 A. Padwa and L. Hamilton, *J. Am. Chem. Soc.*, 1967, **89**, 102; H. Nozaki, S. Fujita, and R. Noyori, *Tetrahedron*, 1968, **24**, 2193; A. Padwa and W. Eisenhardt, *J. Am. Chem. Soc.*, 1971, **93**, 1400; A. G. Anastassiou and R. B. Hammer, *ibid.*, 1972, **94**, 303.
- 3 S. Nishimoto, T. Izukawa, and T. Kagiya, *Bull. Chem. Soc. Jpn.*, 1982, **55**, 1484.
- 4 S. Nishimoto and Y. Nishijima, *Annu. Rep. Res. Inst. Chem. Fibers*, 1975, **32**, 41; S. Ito, M. Yamamoto, and Y. Nishijima, *Bull. Chem. Soc. Jpn.*, 1981, **54**, 35.
- 5 J. G. Calvert and J. N. Pitts, Jr., 'Photochemistry,' Wiley, New York, 1966, p. 783.
- 6 S. Nishimoto, T. Izukawa, and T. Kagiya, *Bull. Chem. Soc. Jpn.*, 1982, **55**, 2937.
- 7 H. A. Benesi and J. H. Hildebrand, *J. Am. Chem. Soc.*, 1949, **71**, 2703.
- 8 R. F. Weimer and J. M. Prausnitz, *J. Chem. Phys.*, 1965, **42**, 3643; L. W. Reeves and W. G. Schneider, *Can. J. Chem.*, 1957, **35**, 251.
- 9 D. Rehm and A. Weller, *Ber. Bunsenges. Phys. Chem.*, 1969, **73**, 834.
- 10 J. G. Calvert and J. N. Pitts, Jr., 'Photochemistry,' Wiley, New York, 1966, p. 298.
- 11 S. P. McGlynn, T. Azumi, and M. Kinoshita, 'Molecular Spectroscopy of the Triplet State,' Prentice-Hall, Englewood Cliffs, 1969, p. 159.

Received 28th October 1982; Paper 2/1824